

## Electronic Supplementary Information

### The efficiency of DPPH as a polarising agent for DNP-NMR spectroscopy

Lloyd Lumata, Matthew Merritt, Chalermchai Khemtong, S. James Ratnakar, Johan van Tol, Lu Yu, Likai Song, and Zoltan Kovacs\*

#### *Table of Contents*

I. W-band ESR spectra of BDPA, DPPH, and 4-oxo-TEMPO at 100 K.....	page S2
II. DPPH electronic magnetisation recovery fitting curves at 100 K and 5 K.....	page S3
III. W-band electronic relaxation of BDPA at 100 K and 5 K.....	page S4
IV. Optimisation of DPPH concentration for DNP.....	page S5
V. $^{13}\text{C}$ microwave DNP spectra of samples doped with DPPH and DPPH-derivative.....	page S6
VI. $^{15}\text{N}$ $T_1$ decay curves of hyperpolarised pentaerythrityl tetraazide.....	page S7
VII. UV/Vis spectroscopy of filtered and unfiltered DPPH solutions.....	page S8
VIII. References.....	page S8

### I. W-band ESR spectra of BDPA, DPPH, and 4-oxo-TEMPO at 100 K

As mentioned in the main text, the ESR properties of the free radicals are crucial elements to the DNP process.<sup>1</sup> As such, we have measured the ESR spectra of the free radicals discussed in this work. Fig. S1 displays the W-band ESR spectra of (a) 1,3-bisdiphenylene-2-phenylallyl (BDPA; 20 mM in 1:1 v/v sulfolane:DMSO), (b) 2,2-diphenyl-1-picrylhydrazyl (DPPH; 20 mM in 1:1 v/v sulfolane:DMSO), and (c) 4-oxo-2,2,6,6-tetramethylpiperidine-1-oxyl (4-oxo-TEMPO; 15 mM in 1:1 glycerol:water) measured at 100 K. It is evident that the DPPH base to base linewidth  $D$  (290 MHz) is intermediate between that of BDPA (62 MHz) and 4-oxo-TEMPO (465 MHz). The ESR spectra of the N-centered DPPH and the nitroxide-based 4-oxo-TEMPO show similar features due to the hyperfine interaction of the paramagnetic electron with the quadrupolar  $^{14}\text{N}$  nuclei. These data at 100 K should reflect the same features of the ESR spectra at DNP conditions (1.4 K).

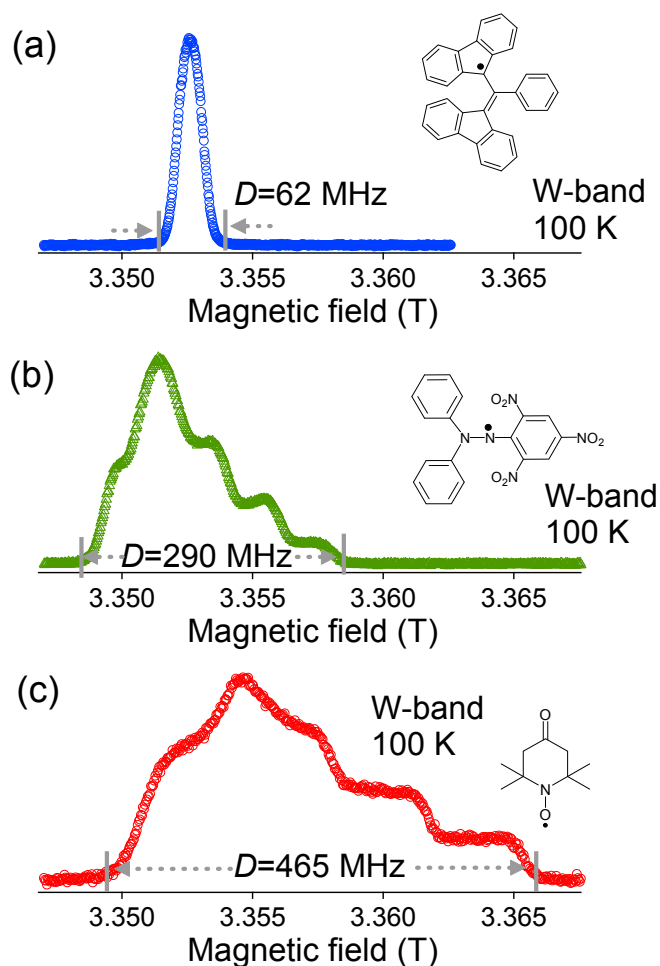


**Fig. S1** W-band ESR spectra of (a) BDPA (20 mM in 1:1 v/v sulfolane:DMSO), (b) DPPH (20 mM in 1:1 v/v sulfolane:DMSO), and (c) 4-oxo-TEMPO (15 mM in 1:1 v/v glycerol:water) measured at 100 K. The insets are the corresponding structures of the free radicals.

## II. DPPH electronic magnetisation recovery fitting curves

Fig. S2 shows the W-band electronic magnetisation recovery curves for 20 mM DPPH at (a) 100 K and (b) 5 K. These relaxation data were fitted to different exponential recovery equations to extract the electron spin-lattice relaxation time  $T_{1e}$ : (i) Single exponential equation  $M_z(t)=M_0[1-\exp(-t/T_{1e})]$ , (ii) stretched exponential equation  $M_z(t)=M_0[1-\exp(-(t/T_{1e})^\beta)]$  where the exponent  $\beta$  is the “stretching” parameter, and (iii) double exponential equation  $M_z(t)=M_0[1-\exp(-t/T_{1e})-\exp(-t/T_{cr})]$  where the longer relaxation component gives the  $T_{1e}$  value and the shorter component  $T_{cr}$  is ascribed to cross relaxation effects.<sup>2</sup> At 100 K, the stretched ( $T_{1e}=0.7783$  ms with  $\beta=0.64$ ) and double ( $T_{1e}=1.87$  ms with  $T_{cr}=0.31$  ms) exponential recovery equations give excellent fits with the data in Fig. S2a whereas the single exponential equation gave a sufficiently good fit with  $T_{1e}=1.13$  ms. However at 5 K, it is evident that a single exponential equation is incompatible with the data. The stretched exponential equations yielded a good fit with the 5 K data which  $T_{1e}=21$  ms but the stretching parameter dropped from 0.64 to 0.24. The double exponential equation gave the best fit to the 5 K data with  $T_{1e}=30.1$  ms and  $T_{cr}=0.43$  ms. This type of relaxation behaviour (bi-exponential electronic magnetisation recovery curve) was also observed in TEMPO (40 mM) at high fields where cross relaxation effects become evident at such relatively high concentration of free radicals.<sup>2</sup>

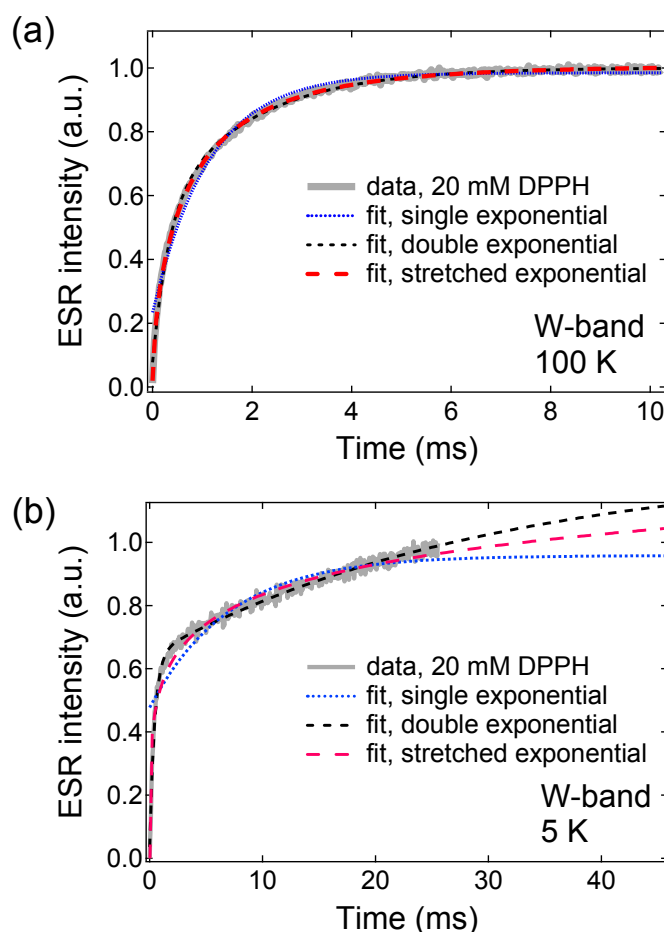


**Fig S2** Recovery curve of the electron magnetisation of 20 mM DPPH in 1:1 sulfolane:DMSO taken at W-band and 5 K. The dashed lines are fits to the data.

### III. W-band electronic relaxation of BDPA

The W-band electronic magnetisation recovery curves of BDPA (20 mM in 1:1 v/v sulfolane:DMSO), shown in Fig. S3, were traced by saturation recovery technique. Similar to the fitting procedure used for DPPH, a single exponential recovery equation did not yield an appropriate fit especially at low temperatures; a double exponential recovery equation was found to be more appropriate where the longer component gives the  $T_{1e}$  value as discussed before. Since the concentration and glassing conditions were the same for both BDPA and DPPH ESR samples, a direct comparison can be made. BDPA has longer electronic  $T_{1e}$ 's than DPPH, with  $T_{1e}$ =21.8 ms at 100 K and  $T_{1e}$ =176 ms at 5 K as shown in Fig. S3; DPPH  $T_{1e}$ =1.87 ms at 100 K and  $T_{1e}$ =30.1 ms at 5 K as illustrated in Fig. S2. This can be qualitatively ascribed to the less g-anisotropy and hyperfine interaction relaxation contribution in BDPA than DPPH.

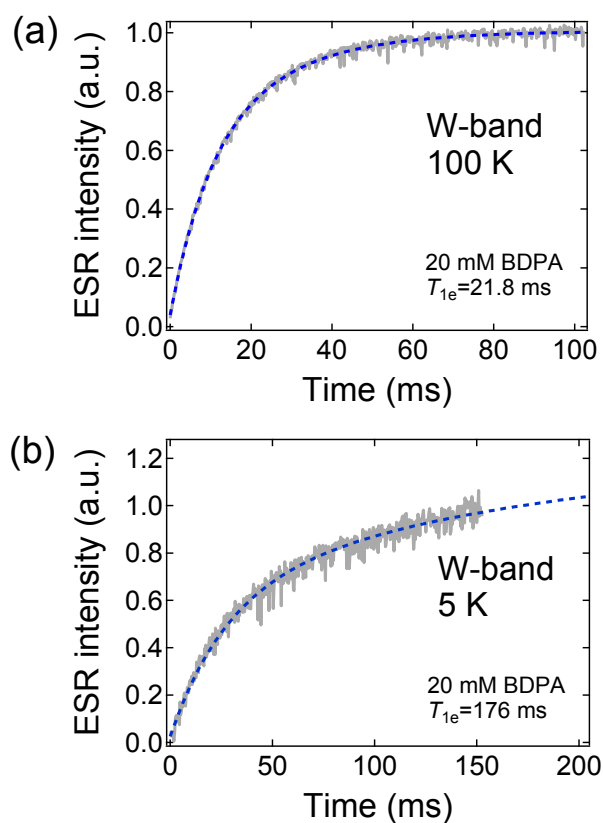


**Fig. S3** W-band electronic magnetisation recovery curves of 20 mM BDPA in 1:1 v/v sulfolane:DMSO measured at (a) 100 K and (b) 5 K. The dashed lines are fits to a double exponential recovery equation where the longer component as described previously.

#### IV. Optimisation of DPPH concentration for DNP

Fig. S4a shows the representative  $^{13}\text{C}$  polarisation buildup curves of 1:1 [ $^{13}\text{C}$ ]ethyl pyruvate:sulfolane doped with the optimum DPPH concentration (20 mM or 40 mM) for DNP at 3.35 T and 1.4 K. A maximum polarisation of ~5 % was achieved for the optimum DPPH-doped sample, whereas the same sample doped with BDPA yielded a  $^{13}\text{C}$  polarisation of 11 %. As mentioned in the main text, the higher polarisation achieved with BDPA is a consequence of its small ESR linewidth  $D$ , which implies that a lower spin temperature of the electron dipolar system can be achieved with DNP via thermal mixing, thus resulting in “colder” spin temperature (higher polarisation) of the nuclear Zeeman system.<sup>1,3</sup> Fig. S4b displays the plot of the dependence of the  $^{13}\text{C}$  polarisation with DPPH concentration where it can be seen that the polarisation is maximum in the concentration range 20-40 mM.

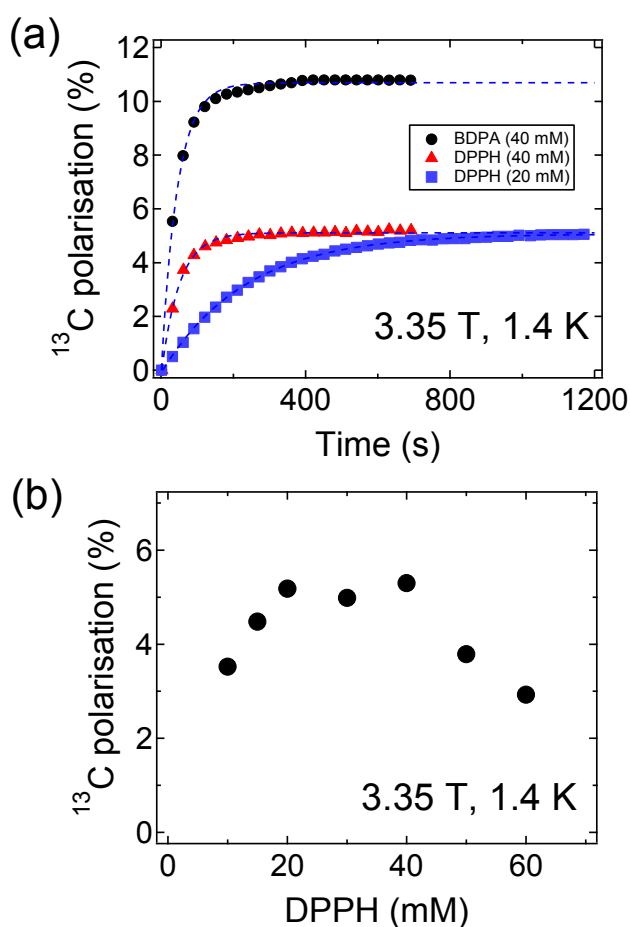


**Fig. S4** (a) Polarisation buildup curves of 1:1 [ $^{13}\text{C}$ ]ethyl acetate:sulfolane doped with the optimum concentrations of DPPH (20 mM or 40 mM) and BDPA (40 mM). (b) Summary of the dependence of  $^{13}\text{C}$  polarisation with DPPH concentration. These data were taken at 3.35 T and 1.4 K.

### V. $^{13}\text{C}$ microwave DNP spectra of samples doped with DPPH and DPPH-derivative

Fig. S5 shows the microwave DNP spectra of 1:1 v/v [ $^{13}\text{C}$ ]ethyl acetate:sulfolane doped with a) 20 mM 2,2-diphenyl-1-picrylhydrazyl (DPPH) and b) 20 mM of a DPPH derivative, 2,2-di(4-tert-octylphenyl)-1-picrylhydrazyl. These data were taken in the HyperSense at 3.35 T and 1.4 K with a 100 mW microwave source. The features of the  $^{13}\text{C}$  DNP spectra are nearly identical for both free radicals; a slight shift up in frequency (downfield shift) was observed for the DPPH-derivative due to the chemical modifications made in the phenyl groups.

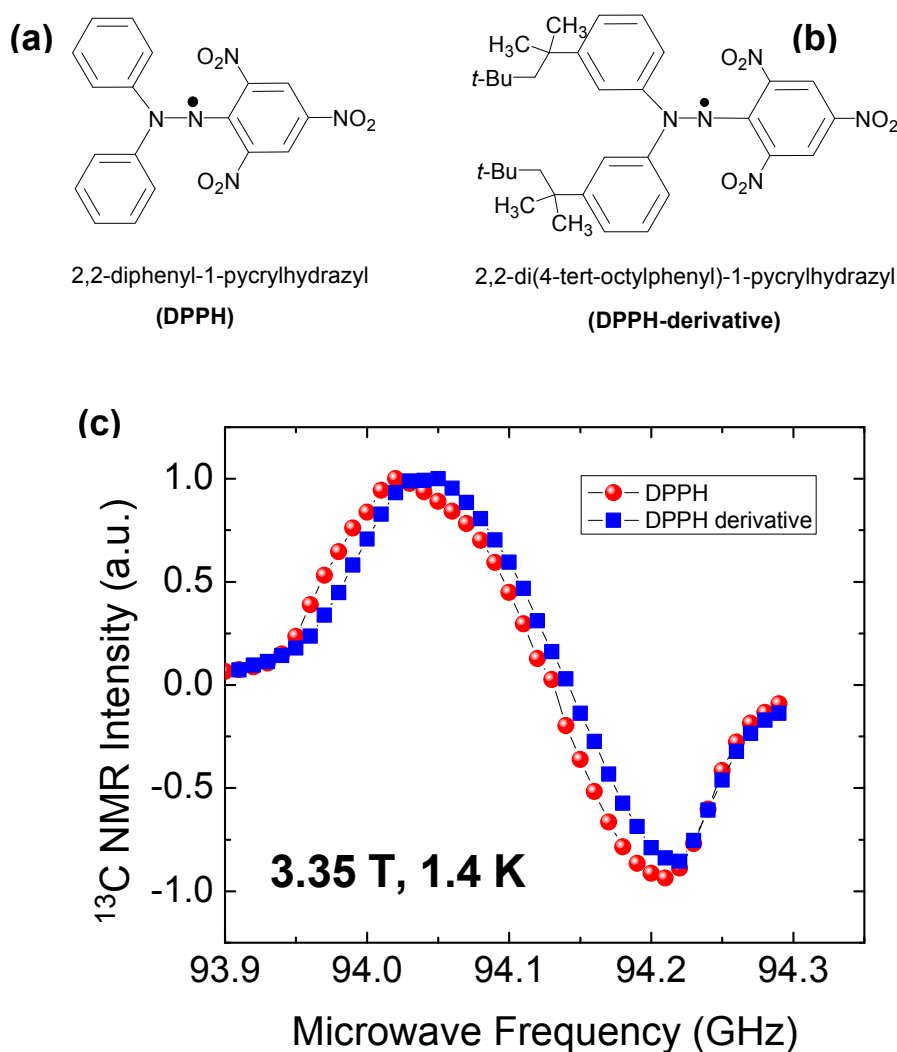


**Fig. S5** Structures of (a) 2,2-diphenyl-1-picrylhydrazyl (DPPH) and (b) a DPPH derivative 2,2-di(4-tert-octylphenyl)-1-picrylhydrazyl. (c)  $^{13}\text{C}$  microwave DNP spectra of 1:1 v/v [ $^{13}\text{C}$ ]ethyl acetate:sulfolane doped with DPPH (20 mM) and a DPPH derivative (20 mM; see structure in Figure 1b). These data were taken at 3.35 T and 1.4 K with a 100 mW microwave source.

## VI. $^{15}\text{N}$ $T_1$ decay curves of hyperpolarised pentaerythrityl tetraazide

In fast dissolution DNP-NMR, long spin-lattice relaxation time  $T_1$  translates to long lifetime of the hyperpolarised state. Fig. S6 shows the decay of the hyperpolarised  $^{15}\text{N}$  NMR signals emanating from the  $\text{CH}_2$ -linked, central, and terminal  $^{15}\text{N}$  (natural abundance) nuclei of pentaerythrityl tetraazide in methanol solution. These data were collected at 9.4 T and 298 K. The decay of the hyperpolarised signal was monitored by applying a small rf detection pulse with flip angle  $\theta_{\text{flip}}=5^\circ$  every time interval  $\text{TR}=10$  s. To extract the  $T_1$  values, the data were fitted to the equation:<sup>4</sup>

$$M_z(t) = M_0 \sin\theta_{\text{flip}} (\cos\theta_{\text{flip}})^{t/\text{TR}} \exp(-t/T_1)$$

where  $M_0$  is the original magnetisation prior to rf pulsing. This equation accounts for the loss of magnetisation due to rf excitation and  $T_1$  relaxation.

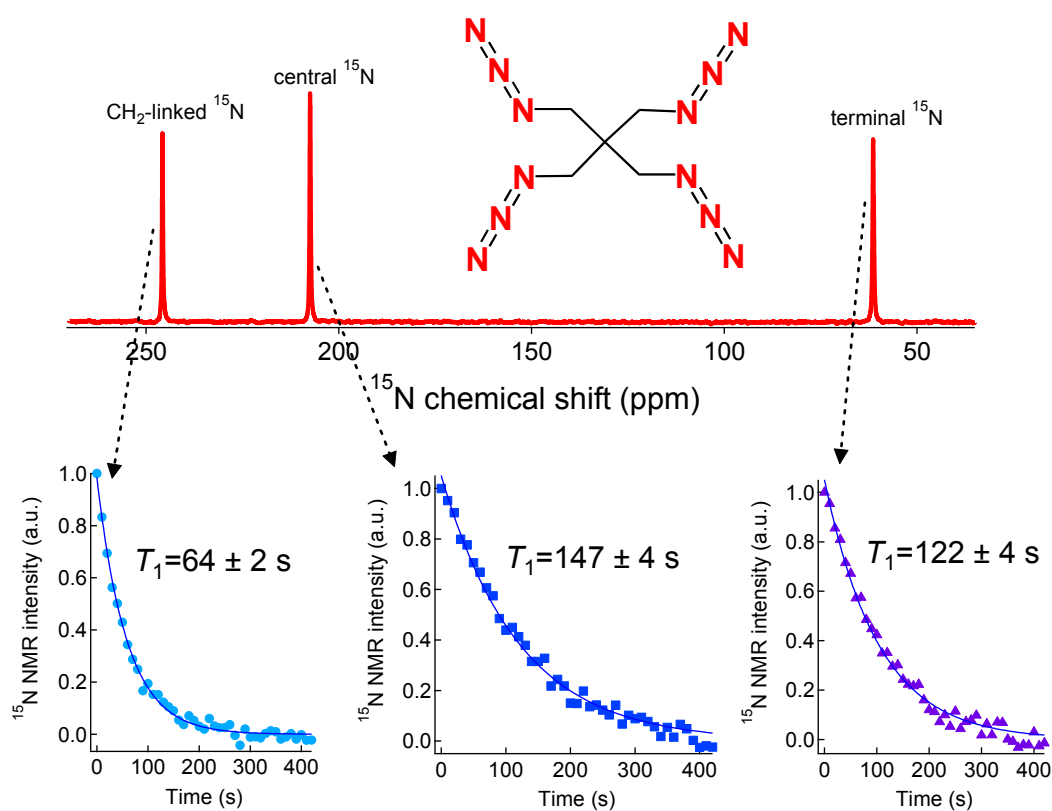


**Fig. S6** Decay of the hyperpolarised  $^{15}\text{N}$  NMR signals from the  $\text{CH}_2$ -linked, central, and terminal  $^{15}\text{N}$  (natural abundance) nuclei of pentaerythrityl tetraazide (31 mM in methanol). These measurements were taken at 9.4 T and 298 K. The decay of the hyperpolarised signal was monitored by applying a 5-degree detection pulse every 10 s.

## VII. UV/Vis spectroscopy of filtered and unfiltered DPPH solutions

Similar to the fast dissolution DNP of BDPA-doped samples,<sup>3</sup> the hydrophobic DPPH free radical can be easily removed from aqueous dissolution liquids by a simple mechanical filtration process. Fig. S7 shows the UV/Vis spectra of varying DPPH concentration in methanol solution and the filtered aqueous dissolution liquid showing the absence of DPPH after filtration using a 0.2-micron syringe filter. The preparation of radical-free hyperpolarised solution is an important attribute for future *in vivo* magnetic resonance spectroscopy or imaging experiments.

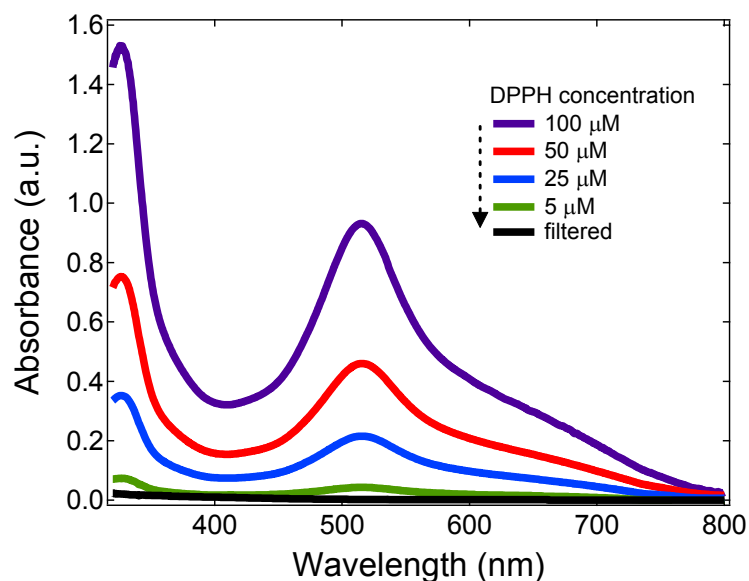


**Fig. S7** UV/Vis spectra of varying DPPH concentration in methanol solution and the filtered aqueous dissolution liquid.

## VIII. References

- [1] J. Heckmann, W. Meyer, E. Radtke, G. Reicherz and S. Goertz, *Phys. Rev. B*, 2006, **74**, 134418.
- [2] C. T. Farrar, D. A. Hall, G. J. Gerfen, S. J. Inati and R. G. Griffin, *J. Chem. Phys.*, 2001, **114**, 4922.
- [3] L. Lumata, S. J. Ratnakar, A. Jindal, M. Merritt, C. Malloy, A. D. Sherry and Z. Kovacs, *Chem. Eur. J.*, 2011, **17**, 10825-10827.
- [4] B. R. Patyal, J. H. Gao, R. F. Williams, J. Roby, B. Saam, B. A. Rockwell, R. J. Thomas, D. J. Stolarski and P. T. Fox, *J. Magn. Reson.*, 1997, **26**, 58.